HyNTP: An Adaptive Hybrid Network Time Protocol for Clock Synchronization in Heterogeneous Distributed Systems

Marcello Guarro and Ricardo G. Sanfelice

Abstract— **This paper presents HyNTP, a distributed hybrid algorithm that synchronizes the time and rate of a set of clocks connected over a network. Clock measurements of the nodes are given at aperiodic time instants and the controller at each node uses these measurements to achieve synchronization. Due to the continuous and impulsive nature of the clocks and the network, we introduce a hybrid system model to effectively capture the dynamics of the system and proposed hybrid algorithm. Moreover, the HyNTP algorithm allows each agent to estimate the skew of its internal clock in order to allow for synchronization to a common timer rate. We provide sufficient conditions guaranteeing synchronization of the timers, exponentially fast. Numerical results illustrate the synchronization property induced by the proposed algorithm as well as robustness to communication noise.**

I. Introduction

Accurate and reliable clock synchronization has been a growing topic of importance in recent years due to the increased use of packet-switched networks in time-critical distributed applications. The low cost, ease of implementation, and resiliency to changes in network topography of packet-switched networks have led to their adoption in a variety of non-traditional system settings such as robotic swarms, automated manufacturing, distributed optimization, among many others, see [1]. The discrete nature of the network communication and the reliance on dynamical models for control and estimation requires consensus among the distributed agents on a shared time scale. In fact, it is not realistic to assume that consensus on time is for free when the distributed system is subjected to network imperfections such as noise, delay, and jitter. It is therefore paramount that distributed systems employ clock synchronization schemes to establish and maintain the required time consensus for their algorithms.

A common and natural approach to clock synchronization is to use reference-based algorithms where the network agents synchronize to a known reference that is either injected or provided by a leader agent. One such algorithm of this kind is the seminal Networking Time Protocol (NTP) presented in [2] that has been widely used due to its simplicity and ease of implementation. However, algorithms like NTP were designed for relatively static network environments with a defined hierarchy and are most times unfit for applications with dynamic network topologies. Other centralized approaches, such as those shown in the works of [3] and [4], consider a least-squares minimization to synchronize with an elected reference. Unfortunately, these approaches suffer robustness issues when communication with the reference node fails or if the random delays in the transmission are not Gaussian distributed, see [5].

The noted discrepancies in the robustness of the centralized approaches have recently motivated consensus-based solutions that do not rely on a designated reference. In the work of [1], [6] and more recently [7], average consensus protocols are considered that result in asymptotic synchronization of the network clocks. However, these approaches suffer from computational complexity in both memory allocation and execution of the algorithm. Moreover, a high number of iterations is often required before the desired synchronization accuracy is achieved. The work of [8] and [9] also provide asymptotic results using a proportional-integral (PI) consensus algorithm. Though the PI consensus algorithm provides faster convergence than the other approaches using average consensus, the PI algorithm still requires a large number of iterations before synchronization is achieved.

This paper presents HyNTP, a distributed hybrid algorithm that exponentially synchronizes a set of clocks connected over a network. Clock measurements of the nodes are given at aperiodic time instants, and each node uses these measurements to achieve synchronization. Inspired by consensus algorithms in [10], this paper introduces a hybrid system model of a network with continuous and impulsive dynamics that uses a hybrid algorithm to synchronize the network clocks in the presence of non-ideal clock skews. The algorithm also allows for the estimation of the skew of the internal clock at each agent to achieve synchronization with a common rate of change for the timers. The use of a hybrid systems model to solve the problem under consideration allows for the application of a Lyapunov-based analysis to show stability of a desired set of interest. Using results from [11], we show that, via a suitable change of coordinates, our distributed hybrid clock synchronization algorithm guarantees the synchronization configuration of the timers, exponentially fast.

This paper is organized as follows. Section II presents preliminary material on graph theory and hybrid systems. Section III introduces the clock synchronization problem and the system being studied, an outline of the algorithm under consideration, and the associated hybrid model of the closed-loop system. Section IV has the main results. Section V provides numerical examples. Due to space constraints,

This research has been partially supported by the National Science Foundation under Grant no. ECS-1710621, and Grant no. CNS-1544396, by the Air Force Office of Scientific Research under Grant no. FA9550-16-1-0015, Grant no. FA9550-19-1-0053, and Grant no. FA9550-19-1-0169, and by CITRIS and the Banatao Institute at the University of California.

Marcello Guarro and Ricardo G. Sanfelice are with Department of Electrical and Computer Engineering, University of California, Santa Cruz. Email: `mguarro@ucsc.edu, ricardo@ucsc.edu`

the proofs of several results along with other details will be published elsewhere.

Notation: The set of natural numbers including zero, i.e., $\{0, 1, 2, \ldots\}$ is denoted by $\mathbb{N}$. The set of natural numbers is denoted as $\mathbb{N}_{>0}$, i.e., $\mathbb{N}_{>0} = \{1, 2, \ldots\}$. The set of real numbers is denoted as $\mathbb{R}$. The set of non-negative real numbers is denoted by $\mathbb{R}_{\geq 0}$, i.e., $\mathbb{R}_{\geq 0} = [0, \infty)$. The n-dimensional Euclidean space is denoted $\mathbb{R}^n$. Given sets A and B, $F : A \rightrightarrows B$ denotes a set-valued map from A to B. For a matrix $A \in \mathbb{R}^{n\times m}$, A^T denotes the transpose of A. Given a vector $x \in \mathbb{R}^n$, $|x|$ denotes the Euclidean norm. Given two vectors $x \in \mathbb{R}^n$ and $y \in \mathbb{R}^m$, we use the equivalent notation $(x, y) = [x^\mathsf{T}\ \ y^\mathsf{T}\ ]^\mathsf{T}$. Given a matrix $A \in \mathbb{R}^n$, $|A| := \max\{\sqrt{|\lambda|} : \lambda \in \text{eig}(A^\mathsf{T}A)\}$. For two symmetric matrices $A \in \mathbb{R}^n$ and $B \in \mathbb{R}^n$, $A \succ B$ means that $A-B$ is positive definite; conversely, $A \prec B$ means that $A - B$ is negative definite. Given a function $f : \mathbb{R}^n \to \mathbb{R}^m$, the range of f is given by rge $f := \{y\ :\ \exists\ x \text{ s.t. } y = f(x)\}$. A vector of N ones is denoted $\mathbf{1}_N$. Given a closed set $A \subset \mathbb{R}^n$ and a closed set $B \subset A$, the projection of A onto B is denoted by $\text{proj}_B(A)$. The matrix I_n is used to denote the identity matrix of size $n \times n$.

II. Preliminaries

A. Preliminaries on Graph Theory

Let $\mathcal{G} = (\mathcal{V}, \mathcal{E}, A)$ be a weighted directed graph (digraph) where $\mathcal{V} = \{1, 2, \ldots, n\}$ represents the set of n nodes, $\mathcal{E} \subset \mathcal{V} \times \mathcal{V}$ the set of edges, and $A \in \{0, 1\}^{n\times n}$ represents the adjacency matrix. An edge of $\mathcal{G}$ is denoted by $e_{ij} = (i, j)$. The elements of A are denoted by a_{ij} where $a_{ij} = 1$ if $e_{ij} \in \mathcal{E}$ and $a_{ij} = 0$ otherwise. The in-degree and out-degree of a node i are defined by $d^{in}(i) = \sum_{k=1}^{n} a_{ki}$ and $d^{out}(i) = \sum_{k=1}^{n} a_{ik}$, respectively. The largest and smallest in-degree of a digraph is given by $\bar{d} = \max_{i\in\mathcal{V}} d^{in}(i)$ and $\underline{d} = \min_{i\in\mathcal{V}} d^{in}(i)$. The in-degree matrix is a diagonal matrix denoted $\mathcal{D}$ with elements given by

$$d_{ij} = \begin{cases} d^{in}(i) & \text{if } i = j \\ 0 & \text{if } i \neq j \end{cases} \qquad \forall i \in \mathcal{V}$$

The Laplacian matrix of a digraph $\mathcal{G}$, denoted by $\mathcal{L}$, is defined as $\mathcal{L} = \mathcal{D} - A$ and has the property that $\mathcal{L}\mathbf{1}_n = 0$. The set of nodes corresponding to the neighbors that share an edge with node i is denoted by $\mathcal{N}(i) := \{k \in \mathcal{V}\ :\ e_{ki} \in \mathcal{E}\ \}$. In the context of networks $\mathcal{N}(i)$, this represents the set of nodes for which an agent i can communicate with.

Lemma 2.1: ((Olfati-Saber and Murray, 2004, Theorem 6),(Fax and Murray, 2004, Propositions 1, 3, and 4)) For an undirected graph, $\mathcal{L}$ is symmetric and positive semidefinite and each eigenvalue of $\mathcal{L}$ is real. For a directed graph, zero is a simple eigenvalue of $\mathcal{L}$ if the directed graph is strongly connected.

Lemma 2.2: (Godsil and Royle (2001)) Consider an $n\times n$ symmetric matrix $A = \{a_{ik}\}$ satisfying $\sum_{i=1}^{n} a_{ik} = 0$ for each $k \in \{1, 2, \ldots, n\}$. The following statements hold:

- *There exists an orthogonal matrix U such that $U^\top AU = \begin{bmatrix} 0 & 0 \\ 0 & \star \end{bmatrix}$ where $\star$ represents any nonsingular matrix with appropriate dimensions and 0 represents any zero matrix with appropriate dimensions.*
- *The matrix A has a zero eigenvalue with eigenvector $\mathbf{1}_n \in \mathbb{R}^n$.*

Definition 2.3: A weighted digraph is said to be

- *balanced* if the in-degree matrix and out-degree matrix for every node is equal, i.e., $d^{in}(i) = d^{out}(i)$ for each $i \in \mathcal{V}$.
- *complete* if every pair of distinct nodes is connected by a unique edge, i.e., $a_{ik} = 1$ for each $i, k \in \mathcal{V}, i \neq k$.
- *strongly connected* if and only if for any two distinct nodes there exists a path of directed edges that connects them.

B. Preliminaries on Hybrid Systems

A hybrid system $\mathcal{H}$ in $\mathbb{R}^n$ is composed by the following *data*: a set $C \subset \mathbb{R}^n$, called the flow set; a set-valued mapping $F : \mathbb{R}^n \rightrightarrows \mathbb{R}^n$ with $C \subset \text{dom } F$, called the flow map; a set $D \subset \mathbb{R}^n$, called the jump set; a set-valued mapping $G : \mathbb{R}^n \rightrightarrows \mathbb{R}^n$ with $D \subset \text{dom } G$, called the jump map. Then, a hybrid system $\mathcal{H} := (C, F, D, G)$ is written in the compact form

$$\mathcal{H} \begin{cases} \dot{x} \ \in F(x) & x \in C \\ x^+ \in G(x) & x \in D \end{cases} \tag{1}$$

where x is the system state. In this paper, a single-valued flow map is used and is denoted f. Solutions to hybrid systems are parameterized by (t, j), where $t \in \mathbb{R}_{\geq 0}$ defines ordinary time and $j \in \mathbb{N}$ is a counter that defines the number of jumps. The evolution of ϕ is described by a *hybrid arc* on a *hybrid time domain* [7]. A hybrid time domain is given by dom $\phi \subset \mathbb{R}_{\geq 0} \times \mathbb{N}$ if, for each $(T, J) \in$ dom ϕ, dom $\phi \cap ([0, T] \times \{0, 1, ..., J\})$ is of the form $\bigcup_{j=0}^{J}([t_j, t_{j+1}] \times \{j\})$, with $0 = t_0 \leq t_1 \leq t_2 \leq t_{J+1}$. A solution ϕ is said to be *maximal* if it cannot be extended by flow or a jump, and *complete* if its domain is unbounded. The set of all maximal solutions to a hybrid system $\mathcal{H}$ is denoted by $\mathcal{S}_\mathcal{H}$ and the set of all maximal solutions to $\mathcal{H}$ with initial condition belonging to a set A is denoted by $\mathcal{S}_\mathcal{H}(A)$. A hybrid system is *well-posed* if it satisfies the hybrid basic conditions in [11, Assumption 6.5].

Definition 2.4: Let a hybrid system $\mathcal{H}$ be defined on $\mathbb{R}^n$. Let $\mathcal{A} \subset \mathbb{R}^n$ be closed. The set $\mathcal{A}$ is said to be stable for $\mathcal{H}$ if for every $\varepsilon > 0$ there exists $\delta > 0$ such that every solution ϕ to $\mathcal{H}$ with $|\phi(0, 0)|_\mathcal{A} \leq \delta$ satisfies $|\phi(t, j)|_\mathcal{A} \leq \varepsilon$ for all $(t, j) \in$ dom ϕ.

Definition 2.5: Let a hybrid system $\mathcal{H}$ be defined on $\mathbb{R}^n$. Let $\mathcal{A} \subset \mathbb{R}^n$ be closed. The set $\mathcal{A}$ is said to be globally exponentially stable (GES) for $\mathcal{H}$ if there exist $\kappa, \alpha > 0$ such that every maximal solution ϕ to $\mathcal{H}$ is complete and satisfies $|\phi(t, j)|_\mathcal{A} \leq \kappa e^{-\alpha(t+j)}|\phi(0, 0)|_\mathcal{A}$ for each $(t, j) \in$ dom ϕ.

III. Problem Statement and the HyNTP Algorithm

A. Problem Statement

Consider a group of n sensor nodes connected over a network represented by a digraph $\mathcal{G} = (\mathcal{V}, \mathcal{E}, A)$. Two clocks are attached to each node i of $\mathcal{G}$: an (uncontrollable) internal clock $\tau_i^* \in \mathbb{R}_{\geq 0}$ whose dynamics are given by

$$\dot{\tau}_i^* = a_i \tag{2}$$

and an adjustable clock $\tilde{\tau}_i \in \mathbb{R}_{\geq 0}$ with dynamics

$$\dot{\tilde{\tau}}_i = a_i + u_i \tag{3}$$

where $u_i \in \mathbb{R}$ is a control input.[1] In both of these models, the (unknown) constant a_i represents the drift of the internal clock.

At times t_j for $j \in \mathbb{N}$ (with $t_0 = 0$), node i receives measurements $\tilde{\tau}_k$ from its neighbors. The resulting sequence of time instants $\{t_j\}_{j=1}^{\infty}$ is assumed to be strictly increasing and unbounded. Moreover, for such a sequence, the time elapsed between each time instant when the clock measurements are exchanged is governed by

$$\begin{aligned} &T_1 \leq t_{j+1} - t_j \leq T_2 \qquad \forall j \in \mathbb{N} \setminus \{0\} \\ &0 \leq t_1 \leq T_2 \end{aligned} \tag{4}$$

where $0 < T_1 \leq T_2$, with T_1 defining a minimum time between consecutive measurements and T_2 defines the maximum allowable transfer interval (MATI).

Remark 3.1: The models for the clocks are based on the hardware and software relationship of the real-time system that implements them. That is, the internal clock τ_i^* is treated as a type of hardware oscillator while the adjustable clock $\tilde{\tau}_i$ is treated as a virtual clock, implemented in software (as part of the proposed algorithm), that evolves according to the dynamics of the hardware oscillator. Any virtual clock implemented in node i inherits the drift parameter a_i of the internal clock, which cannot be controlled. More importantly, this drift parameter is not known due to the fact that universal time information is not available to any node.

Under such a setup, our goal is to design a distributed hybrid controller that assigns the input u_i to drive each clock $\tilde{\tau}_i$ to synchronization with every other clock $\tilde{\tau}_j$ and, rather than having $\dot{\tilde{\tau}}_i = a_i$, to have a common prespecified constant rate of change $\sigma^* > 0$ for each clock. This problem is formally stated as follows:

Problem 3.1: Given a network of n agents with dynamics as in (2) and (3) represented by a directed graph $\mathcal{G}$ and $\sigma^* > 0$, design a distributed hybrid controller that achieves the following two properties:

i) Clock synchronization: $\lim_{t\to\infty} |\tilde{\tau}_i(t) - \tilde{\tau}_k(t)| = 0$ for all $i, k \in \mathcal{V}$, $i \neq k$;

ii) Common clock rate: $\lim_{t\to\infty} |\dot{\tilde{\tau}}_i(t) - \sigma^*| = 0$ for all $i \in \mathcal{V}$.

[1] The input u_i is unconstrained as allowed by hardware platforms in practice.

B. The HyNTP Algorithm

We define the hybrid model that provides the framework and a solution to Problem 3.1. First, since we are interested in the ability of the rate of each clock to synchronize to a constant rate σ^*, we propose the following change of coordinates: for each $i \in \mathcal{V}$, define $e_i := \tilde{\tau}_i - r$, where $r \in \mathbb{R}_{\geq 0}$ is such that $\dot{r} = \sigma^*$. The state r is only used for analysis. Then, the dynamics for e_i are given by

$$\dot{e}_i = \dot{\tilde{\tau}}_i - \sigma^* \qquad \forall i \in \mathcal{V} \tag{5}$$

By making the appropriate substitutions, one has

$$\dot{e}_i = a_i + u_i - \sigma^* \qquad \forall i \in \mathcal{V} \tag{6}$$

To model the network dynamics for aperiodic communication events, we consider a timer variable τ with hybrid dynamics

$$\begin{aligned} \dot{\tau} &= -1 & \tau \in [0, T_2] \\ \tau^+ &\in [T_1, T_2] & \tau = 0 \end{aligned} \tag{7}$$

This model is such that when $\tau = 0$, a communication event is triggered, and τ is reset to a point in the interval $[T_1, T_2]$ in order to preserve the bounds given in (4); see [12].

The HyNTP algorithm assigns a value to u_i so as to solve Problem 3.1. The algorithm implements two feedback laws: a distributed feedback law and a local feedback law. The distributed feedback utilizes a control variable $\eta_i \in \mathbb{R}$ that is impulsively updated at communication event times using both local and exchanged measurement information $\tilde{\tau}_k$, i.e., it takes the form

$$\eta_i^+ = \sum_{k \in \mathcal{N}(i)} K_i^k(\tilde{\tau}_i, \tilde{\tau}_k)$$

where $K_i^k(\tilde{\tau}_i, \tilde{\tau}_k) := -\gamma(e_i - e_k)$ with $\gamma > 0$. Between communication event times, η_i evolves continuously. The local feedback strategy utilizes a continuous-time linear adaptive estimator with states $\hat{\tau}_i \in \mathbb{R}$ and $\hat{a}_i \in \mathbb{R}$ to estimate the drift a_i of the internal clock. The estimate of the drift is then injected as feedback to negate the effect of a_i on the evolution of $\tilde{\tau}_i$. Furthermore, the local feedback strategy injects σ^* to give the desired clock rate.

Inspired by the protocol in [10, Protocol 4.1], the dynamics of the i-th hybrid controller are given by

$$\left.\begin{aligned} \dot{u}_i &= 0 \\ \dot{\eta}_i &= h\eta_i \\ \dot{\hat{a}}_i &= -\mu(\hat{\tau}_i - \tau_i^*) \\ \dot{\hat{\tau}}_i &= \hat{a}_i - (\hat{\tau}_i - \tau_i^*) \end{aligned}\right\} \quad \tau \in [0, T_2]$$
$$\left.\begin{aligned} \eta_i^+ &= -\gamma \sum_{k \in \mathcal{N}(i)} (e_i - e_k) \\ u_i^+ &= -\gamma \sum_{k \in \mathcal{N}(i)} (e_i - e_k) - \hat{a}_i + \sigma^* \\ \hat{a}_i^+ &= \hat{a}_i \\ \hat{\tau}_i^+ &= \hat{\tau}_i \end{aligned}\right\} \quad \tau = 0 \tag{8}$$

where $h \in \mathbb{R}$, $\mu > 0$, and $\gamma > 0$ are controller parameters. The state η is included in the model to facilitate a model reduction used in the results that follow. Note that u_i is treated (with some abuse of notation) as an auxiliary state of the controller. This state is kept constant in between events and is reset to the new value of $\eta_i - \hat{a}_i + \sigma^*$ at jumps.

With the timer variable and hybrid controller defined in (8), we construct the hybrid closed-loop system $\mathcal{H} = (C, f, D, G)$ obtained from the interconnection. Let $x = (e, u, \eta, \tau^*, \hat{a}, \hat{\tau}, \tau) \in \mathbb{R}^n \times \mathbb{R}^n \times \mathbb{R}^n \times \mathbb{R}^n \times \mathbb{R}^n \times \mathbb{R}^n \times [0, T_2] =: \mathcal{X}$, where $e = (e_1, e_2, \ldots, e_n)$, $u = (u_1, u_2, \ldots, u_n)$, $\eta = (\eta_1, \eta_2, \ldots, \eta_n)$, $\tau^* = (\tau_1^*, \tau_2^*, \ldots, \tau_N^*)$, $\hat{\tau} = (\hat{\tau}_1, \hat{\tau}_2, \ldots, \hat{\tau}_N)$, $a = (a_1, a_2, \ldots, a_N)$, and $\hat{a} = (\hat{a}_1, \hat{a}_2, \ldots, \hat{a}_n)$. The data (C, f, D, G) of $\mathcal{H}$ is given by

$$f(x) := \begin{bmatrix} a + u - \sigma^* \mathbf{1}_n \\ 0 \\ h\eta \\ a \\ -\mu(\hat{\tau} - \tau^*) \\ \hat{a} - (\hat{\tau} - \tau^*) \\ -1 \end{bmatrix}, \; G(x) := \begin{bmatrix} e \\ -\gamma \mathcal{L} e - \hat{a} + \sigma^* \mathbf{1}_n \\ -\gamma \mathcal{L} e \\ \tau^* \\ \hat{a} \\ \hat{\tau} \\ [T_1, T_2] \end{bmatrix} \tag{9}$$

$C := \mathcal{X}$ and $D := \{x \in \mathcal{X} : \tau = 0\}$.

With the hybrid system defined, the next two results establish the existence of solutions to $\mathcal{H}$ and that every maximal solution to $\mathcal{H}$ is complete. In particular, we show that, through the satisfaction of some basic conditions on the hybrid system data, the system $\mathcal{H}$ is nominally well-posed and that each maximal solution to the system is defined for arbitrarily large $t + j$.

Lemma 3.2: The hybrid system $\mathcal{H}$ satisfies the hybrid basic conditions defined in [11, Assumption 6.5].

Lemma 3.3: For every $\xi \in C \cup D = \mathcal{X}$, every maximal solution ϕ to $\mathcal{H}$ with $\phi(0, 0) = \xi$ is complete.

With the hybrid closed-loop system in (9), the set to asymptotically stabilize so as to solve Problem 3.1 is

$$\mathcal{A} := \{x \in \mathcal{X} : e_i = \eta_i = 0, \hat{a}_i = a_i, \tau_i^* = \hat{\tau}_i \; \forall i \in \mathcal{V}\}$$

Note that $e_i = e_k$ and $\eta_i = 0$ for all $i, k \in \mathcal{V}$ imply synchronization of the clocks, meanwhile $\hat{a}_i = a_i$ and $\tau_i^* = \hat{\tau}_i$ for all $i, k \in \mathcal{V}$ ensure no error in the estimation of the clock skew, and that the internal and estimated clocks are synchronized, respectively. It can be shown that the set $\mathcal{A}$ is forward invariant for the hybrid system $\mathcal{H}$.

IV. Main Results

A. Reduced Model – First Pass

In this section we recast the hybrid system $\mathcal{H}$ into a reduced model obtained by setting $u = \eta - \hat{a} + \sigma^* \mathbf{1}_n$. This model is given in error coordinates for the parameter estimation of the internal clock rate. We let $\varepsilon_a = a - \hat{a}$ denote the estimation error of the internal clock rate and $\varepsilon_\tau = \hat{\tau} - \tau^*$ represent the estimation error of the internal clock state. Then, using this reduced model, we perform a change of coordinates to obtain an auxiliary closed-loop hybrid system model for which asymptotic stability of $\mathcal{A}$ can be assessed. The state of the reduced model is given by $x_\varepsilon := (e, \eta, \varepsilon_a, \varepsilon_\tau, \tau) \in \mathbb{R}^n \times \mathbb{R}^n \times \mathbb{R}^n \times \mathbb{R}^n \times [0, T_2] =: \mathcal{X}_\varepsilon$ with dynamics defined by the data

$$f_\varepsilon(x_\varepsilon) := \begin{bmatrix} \eta + \varepsilon_a \\ h\eta \\ \mu \varepsilon_\tau \\ -\varepsilon_\tau - \varepsilon_a \\ -1 \end{bmatrix}, \quad G_\varepsilon(x_\varepsilon) := \begin{bmatrix} e \\ -\gamma \mathcal{L} e \\ \varepsilon_a \\ \varepsilon_\tau \\ [T_1, T_2] \end{bmatrix}$$

$C_\varepsilon := \mathcal{X}_\varepsilon$ and $D_\varepsilon := \{x_\varepsilon \in \mathcal{X}_\varepsilon : \tau = 0\}$. This system is denoted $\mathcal{H}_\varepsilon = (C_\varepsilon, f_\varepsilon, D_\varepsilon, G_\varepsilon)$. Note that the construction $u = \eta - \hat{a} + \sigma^* \mathbf{1}_n$, which holds along all solutions after the first jump, leads to $\dot{e} = \eta + \varepsilon_a$.

Observe that the state of $\mathcal{H}_\varepsilon$ utilizes most of the state components of $\mathcal{H}$ except for the control input u as it's value is captured by the states η and ε directly in the dynamics of e.

With the reduced model $\mathcal{H}_\varepsilon$ in place, we consider the following set to asymptotically stabilize for $\mathcal{H}_\varepsilon$

$$\mathcal{A}_\varepsilon := \{x_\varepsilon \in \mathcal{X}_\varepsilon : e_i = \eta_i = 0 \; \forall i \in \mathcal{V}, \varepsilon_a = 0, \varepsilon_\tau = 0\}$$

This set is equivalent to $\mathcal{A}$ but given in the error coordinates x_ε.

B. Reduced Model – Second Pass

Global exponential stability of $\mathcal{A}_\varepsilon$ for $\mathcal{H}_\varepsilon$ is established by performing a Lyapunov analysis on a version of $\mathcal{H}_\varepsilon$ obtained after an appropriate change of coordinates, one where the flow and jump dynamics are linearized. The model is obtained by exploiting an important property of the eigenvalues of the Laplacian matrix for strongly connected digraphs. To this end, let $\mathcal{G}$ be a strongly connected digraph. By Lemmas 2.1 and 2.2, there exists a nonsingular matrix $\mathcal{T} = [\mathbf{1}_N, \mathcal{T}_1]$, $\mathcal{T}_1 \in \mathbb{R}^{N \times N-1}$ such that $\mathcal{T}^{-1} \mathcal{L} \mathcal{T} = \begin{bmatrix} 0 & 0 \\ 0 & \bar{\mathcal{L}} \end{bmatrix}$ where $\mathcal{L}$ is the graph laplacian of $\mathcal{G}$ and $\bar{\mathcal{L}}$ is a diagonal matrix with the positive eigenvalues of $\mathcal{L}$ as the diagonal elements given by $(\lambda_2, \lambda_3, \ldots, \lambda_N)$, see [13], [14], and [15] for more details.

To perform the change of coordinates, we use $\mathcal{T}$ to first perform the following transformations: $\bar{e} = \mathcal{T}^{-1} e$, $\bar{\eta} = \mathcal{T}^{-1} \eta$, $\bar{\varepsilon}_a = \mathcal{T}^{-1} \varepsilon_a$ and $\bar{\varepsilon}_\tau = \mathcal{T}^{-1} \varepsilon_\tau$. Then, we define vectors $\bar{z} = (\bar{z}_1, \bar{z}_2)$ and $\bar{w} = (\bar{w}_1, \bar{w}_2)$, where $\bar{z}_1 := (\bar{e}_1, \bar{\eta}_1)$, $\bar{z}_2 := (\bar{e}_2, \ldots, \bar{e}_N, \bar{\eta}_2, \ldots, \bar{\eta}_N)$, $\bar{w}_1 = (\bar{\varepsilon}_{a_1}, \bar{\varepsilon}_{\tau_1})$, and $\bar{w}_2 = (\bar{\varepsilon}_{a_2}, \ldots, \bar{\varepsilon}_{a_n}, \bar{\varepsilon}_{\tau_2}, \ldots, \bar{\varepsilon}_{\tau_n})$. Finally, we define $\chi_\varepsilon := (\bar{z}_1, \bar{z}_2, \bar{w}_1, \bar{w}_2, \tau) \in \mathbb{R}^2 \times \mathbb{R}^{2(n-1)} \times \mathbb{R}^2 \times \mathbb{R}^{2(n-1)} \times [0, T_2] =: \mathcal{X}_{\underset{\sim}{\varepsilon}}$ as the state of the new version of $\mathcal{H}_\varepsilon$, which is denoted $\tilde{\mathcal{H}}_\varepsilon$ and has data given by

$$\tilde{f}_\varepsilon(\chi_\varepsilon) := \begin{bmatrix} A_{f_1} \bar{z}_1 \\ A_{f_2} \bar{z}_2 \\ A_{f_3} \bar{w}_1 \\ A_{f_4} \bar{w}_2 \\ -1 \end{bmatrix} + \begin{bmatrix} B_{f_1} \bar{w}_1 \\ B_{f_2} \bar{w}_2 \\ 0 \\ 0 \\ 0 \end{bmatrix}, \; \tilde{G}_\varepsilon(\chi_\varepsilon) := \begin{bmatrix} A_{g_1} \bar{z}_1 \\ A_{g_2} \bar{z}_2 \\ \bar{w}_1 \\ \bar{w}_2 \\ [T_1, T_2] \end{bmatrix} \tag{10}$$

$\tilde{C}_\varepsilon := \mathcal{X}_\varepsilon$ and $\tilde{D}_\varepsilon := \{\chi_\varepsilon \in \mathcal{X}_\varepsilon : \tau = 0\}$ where

$$A_{f_1}=\begin{bmatrix}0 & 1\\ 0 & h\end{bmatrix}, \quad A_{f_2}=\begin{bmatrix}0 & I_m\\ 0 & hI_m\end{bmatrix}, \quad A_{f_3}=\begin{bmatrix}0 & \mu\\ -1 & -1\end{bmatrix}$$
$$A_{f_4}=\begin{bmatrix}0 & \mu I_m\\ -I_m & -I_m\end{bmatrix}, \quad B_{f_1}=\begin{bmatrix}1 & 0\\ 0 & 0\end{bmatrix}, \quad B_{f_2}=\begin{bmatrix}I_m & 0\\ 0 & 0\end{bmatrix}$$
$$A_{g_1}=\begin{bmatrix}1 & 0\\ 0 & 0\end{bmatrix}, \quad A_{g_2}=\begin{bmatrix}I_m & 0\\ -\gamma\bar{\mathcal{L}} & 0\end{bmatrix}$$

where $m = N - 1$. Then, $\widetilde{\mathcal{H}}_\varepsilon = (\tilde{C}_\varepsilon, \tilde{f}_\varepsilon, \tilde{D}_\varepsilon, \tilde{G}_\varepsilon)$ denotes the new version of $\mathcal{H}_\varepsilon$. The set $\mathcal{A}_\varepsilon$ to stabilize in the new coordinates for this hybrid system is given by

$$\tilde{\mathcal{A}}_\varepsilon := \{\chi_\varepsilon \in \mathcal{X}_\varepsilon : \bar{z}_1{=}(e^*, 0), \bar{z}_2{=}0, \bar{w}_1{=}0, \bar{w}_2{=}0, e^* \in \mathbb{R}\} \tag{11}$$

In the next result, we demonstrate how global exponential stability of $\tilde{\mathcal{A}}_\varepsilon$ for $\widetilde{\mathcal{H}}_\varepsilon$ implies global exponential stability of $\mathcal{A}_\varepsilon$ for $\mathcal{H}_\varepsilon$. This is accomplished by exploiting the relationship that exists between the two systems through the transformation matrix $\mathcal{T}$ on the sets $\tilde{\mathcal{A}}_\varepsilon$ and $\mathcal{A}_\varepsilon$.

Lemma 4.1: Given $0 < T_1 \le T_2$ and a strongly connected digraph $\mathcal{G}$, the set $\tilde{\mathcal{A}}_\varepsilon$ is GES for the hybrid system $\widetilde{\mathcal{H}}_\varepsilon$ if and only if $\mathcal{A}_\varepsilon$ is GES for the hybrid system $\mathcal{H}_\varepsilon$.

C. Parameter Estimator

Exponential stability of the set $\tilde{\mathcal{A}}_\varepsilon$ for $\widetilde{\mathcal{H}}_\varepsilon$ hinges upon the convergence of the estimate $\hat{a}$ to a. We present a result establishing convergence of $\hat{a}$ to a by considering a reduction of $\widetilde{\mathcal{H}}_\varepsilon$. To this end, consider the state $\chi_{\varepsilon_r} := (\bar{w}_1, \bar{w}_2, \tau) \in \mathbb{R}^2 \times \mathbb{R}^{2(n-1)} \times [0, T_2] =: \mathcal{X}_{\varepsilon_r}$. Its dynamics are given by the system $\widetilde{\mathcal{H}}_{\varepsilon_r} = (\tilde{C}_{\varepsilon_r}, \tilde{f}_{\varepsilon_r}, \tilde{D}_{\varepsilon_r}, \tilde{G}_{\varepsilon_r})$ with data

$$\tilde{f}_{\varepsilon_r}(\chi_{\varepsilon_r}) := \begin{bmatrix}A_{f_3}\bar{w}_1\\ A_{f_4}\bar{w}_2\\ -1\end{bmatrix} \quad \tilde{G}_{\varepsilon_r}(\chi_{\varepsilon_r}) := \begin{bmatrix}\bar{w}_1\\ \bar{w}_2\\ [T_1, T_2]\end{bmatrix}$$

$\tilde{C}_{\varepsilon_r} := \mathcal{X}_{\varepsilon_r}$ and $\tilde{D}_{\varepsilon_r} := \{\chi_{\varepsilon_r} \in \mathcal{X}_{\varepsilon_r} : \tau{=}0\}$. For this system, the set to exponentially stabilize for the reduced hybrid system $\widetilde{\mathcal{H}}_{\varepsilon_r}$ is given by

$$\tilde{\mathcal{A}}_{\varepsilon_r} := \{0\} \times \{0\} \times [0, T_2] \tag{12}$$

In the next result, we show global exponential stability of the set $\tilde{\mathcal{A}}_{\varepsilon_r}$ for $\widetilde{\mathcal{H}}_{\varepsilon_r}$ through the satisfaction of matrix inequalities.

Proposition 4.2: Let $0 < T_1 \le T_2$ be given. If there exist a positive scalar μ and positive definite symmetric matrices P_2, P_3 such that

$$P_2 A_{f_3} + A_{f_3}^\top P_2 \prec 0 \tag{13}$$
$$P_3 A_{f_4} + A_{f_4}^\top P_3 \prec 0 \tag{14}$$

hold, then the set $\tilde{\mathcal{A}}_{\varepsilon_r}$ is globally exponentially stable for the hybrid system $\widetilde{\mathcal{H}}_{\varepsilon_r}$. Furthermore, every solution ϕ to $\widetilde{\mathcal{H}}_{\varepsilon_r}$ satisfies

$$|\phi(t,j)|_{\tilde{\mathcal{A}}_{\varepsilon_r}} \le \sqrt{\frac{\alpha_2}{\alpha_1}} \exp\Big(-\frac{\tilde{\beta}}{2\alpha_2} t\Big) |\phi(0,0)|_{\tilde{\mathcal{A}}_{\varepsilon_r}} \tag{15}$$

for each $(t,j) \in dom\ \phi$, with $\alpha_1 = \min\{\lambda_{min}(P_2), \lambda_{min}(P_3)\}$ $\alpha_2 = \max\{\lambda_{max}(P_2), \lambda_{max}(P_3)\}$ and $\tilde{\beta} > 0$.

D. Exponential Stability of Reduced Model $\widetilde{\mathcal{H}}_\varepsilon$

With the convergence of the clock rate parameter estimation established, we introduce our main result. We show globally exponential stability of the set $\mathcal{A}_\varepsilon$ for the closed-loop hybrid system $\mathcal{H}_\varepsilon$ via an analysis of the auxiliary system $\widetilde{\mathcal{H}}_\varepsilon$ and its global exponential stability for the auxiliary set $\tilde{\mathcal{A}}_\varepsilon$ in (11).

Theorem 4.3: Given a strongly connected digraph $\mathcal{G}$, if the parameters $T_2 \ge T_1 > 0$, $\mu > 0$, $h \in \mathbb{R}$, and $\gamma > 0$, the positive definite matrices P_1, P_2, and P_3 are such that conditions (13), (14), and

$$A_{g_2}^\top \exp(A_{f_2}^\top \nu) P_1 \exp(A_{f_2}\nu) A_{g_2} - P_1 \prec 0 \quad \forall \nu \in [T_1, T_2] \tag{16}$$
$$\Big|\exp\Big(\frac{\bar{\kappa}_1}{\alpha_2} T_2\Big)\Big(1 - \frac{\bar{\kappa}_2}{\alpha_2}\Big)\Big| < 1 \tag{17}$$

hold, where

$$\bar{\kappa}_1 = \max\Big\{\frac{\kappa_1}{2\epsilon}, \frac{\kappa_1 \epsilon}{2} - \beta_2\Big\}$$
$$\kappa_1 = 2 \max_{v \in [0, T_2]} \big|\exp(A_{f_2}^\top v) P_1 \exp(A_{f_2} v)\big|$$
$$\bar{\kappa}_2 = \min\{1, \kappa_2\}$$
$$\kappa_2 \in \Big(0, -\big(\min_{v \in [T_1, T_2]} \lambda_{min}(A_{g_2}^\top \exp(A_{f_2}^\top v) P_1 \exp(A_{f_2} v) A_{g_2} - P_1)\big)\Big)$$
$$\alpha_2 = \max_{s \in [0, T_2]} \Big\{\exp(2hs), \lambda_{max}\big(\exp(A_{f_2}^\top s) P_1 \exp(A_{f_2} s)\big), \lambda_{max}(P_2), \lambda_{max}(P_3)\Big\}$$

$P_2 A_{f_3} + A_{f_3}^\top P_2 \le -\beta_1 I$, and $P_3 A_{f_4} + A_{f_4}^\top P_3 \le -\beta_2 I$ for some $\epsilon > 0$ then, the set $\tilde{\mathcal{A}}_\varepsilon$ in (11) is globally exponentially stable for the hybrid system $\widetilde{\mathcal{H}}_\varepsilon$ in (10).

Though the details of the result have been omitted due to space constraints, we note to the reader that the conditions for which GES of $\tilde{\mathcal{A}}_\varepsilon$ for $\widetilde{\mathcal{H}}_\varepsilon$ is guaranteed can be established via the following Lyapunov function candidate

$$V(\chi_\varepsilon) = V_1(\chi_\varepsilon) + V_2(\chi_\varepsilon) + V_{\varepsilon_r}(\chi_\varepsilon) \tag{18}$$

where

$$V_1(\chi_\varepsilon) = \exp(2h\tau)\bar{\eta}_1^2 \qquad V_{\varepsilon_r}(\chi_\varepsilon) = \bar{w}_1^\top P_2 \bar{w}_1 + \bar{w}_2^\top P_3 \bar{w}_2$$
$$V_2(\chi_\varepsilon) = \bar{z}_2^\top \exp(A_{f_2}^\top \tau) P_1 \exp(A_{f_2}\tau) \bar{z}_2$$

Moreover, since the result establishes GES of $\mathcal{A}_\varepsilon$ for $\mathcal{H}_\varepsilon$, we have that solutions for $\mathcal{H}$ converge to $\mathcal{A}$, exponentially fast; hence, Problem 3.1 is solved.

V. Numerical Results

Example 5.1: Consider five agents with dynamics as in (2) and (3) over a strongly connected graph with the following adjacency matrix

$$\mathcal{G}_A = \begin{pmatrix}0 & 1 & 1 & 0 & 1\\ 1 & 0 & 1 & 0 & 0\\ 1 & 0 & 0 & 1 & 0\\ 0 & 0 & 1 & 0 & 1\\ 1 & 0 & 1 & 1 & 0\end{pmatrix}$$

Given $T_1 = 0.01$, $T_2 = 0.1$, and $\sigma^* = 1$, then it can be found that the parameters $h = -1.3$, $\mu = 3$, $\gamma =$

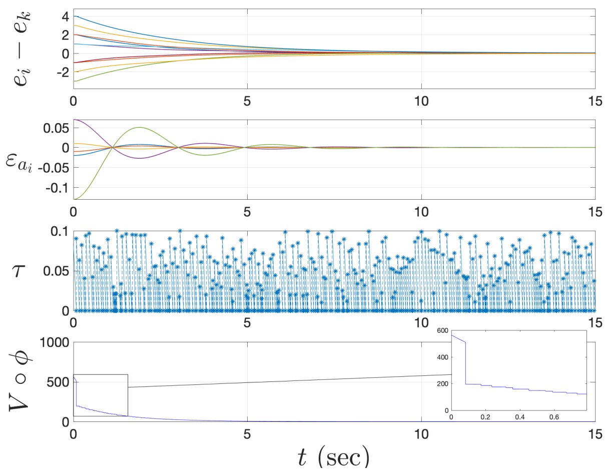

Fig. 1. The trajectories of the state component errors $e_i - e_k$, ε_{a_i}, and τ for $i \in \{1, 2, 3, 4, 5\}$ of the solution ϕ for the case where $\sigma = \sigma^*$. Plot of V from (18) evaluated along the solution ϕ projected onto the regular time domain. (bottom)

0.125 and $\epsilon = 1.607$ with suitable matrices P_1, P_2, and P_3 satisfy conditions (16) and (17) in Theorem 4.3 with $\bar{\kappa}_1 = 9.78$, $\kappa_1 = 31.44$, $\bar{\kappa}_2 = 1$, and $\alpha_2 = 18.923$. Figure 1 shows the trajectories of $e_i - e_k$, ε_{a_i} for components $i \in \{1, 2, 3, 4, 5\}$ of a solution ϕ for the case where $\sigma = \sigma^*$ with initial conditions $\phi_e(0, 0) = (1, -1, 2, -2, 0)$, $\phi_\eta(0, 0) = (0, -3, 1, -4, -1)$, and clock rates a_i in the range $(0.85, 1.15)$. [2]

Example 5.2: In this example we demonstrate by simulation the system's robustness to noise on the communication channel and the clock rate reference σ^*. Consider the same system presented in Example 5.1. Figure 2 shows input-to-state stability for the trajectories of the errors $e_i - e_k$ for the components $i \in \{1, 2, 3, 4, 5\}$ of a solution ϕ for the case where the system is subjected to communication noise $m_{e_i}(t, j) \in (0, 0.1)$ and noise on the clock rate reference $m_{\sigma_i^*}(t, j) \in (0.85, 1.15)$ for all $(t, j) \in \operatorname{dom} \phi$, respectively. Moreover, after the respective transient period, the norm of the relative error $|e_i - e_k|$ converges to an average value of 0.0229 when subjected to noise $m_{\sigma_i^*}$ and 0.0549 for noise m_{e_i}.

VI. Conclusion

In this paper, we modeled a network of clocks with aperiodic communication that utilizes the presented HyNTP algorithm to achieve synchronization, using the hybrid systems framework. Results were given to guarantee and show synchronization of the timers, exponentially fast. Numerical results validating the exponentially fast convergence of the timers were also given. Numerical results were also provided regarding its robustness to a class of perturbations. Future work will demonstrate the algorithm's robustness to a variety of perturbations and extend the problem to the case of asynchronous broadcasts between the nodes. Consideration will also be given to the scenario of time-varying clock skew parameters.

[2]Code at github.com/HybridSystemsLab/HybridClockSync

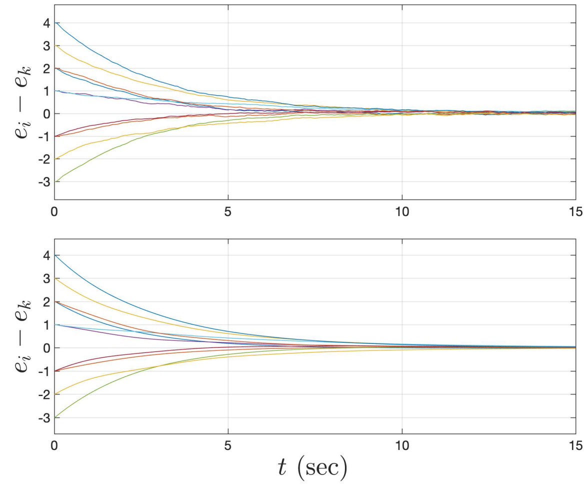

Fig. 2. (top) The trajectories of the errors $e_i - e_k$ for the components $i \in \{1, 2, 3, 4, 5\}$ of a solution ϕ for the case where the system is subjected to communication noise m_{e_i} (top) and noise on the clock rate reference $m_{\sigma_i^*}$ (bottom).

References

[1] L. Schenato and F. Fiorentin, "Average timesynch: A consensus-based protocol for clock synchronization in wireless sensor networks," *Automatica*, vol. 47, no. 9, pp. 1878–1886, 2011.

[2] D. L. Mills, "Internet time synchronization: the network time protocol," *IEEE Transactions on communications*, vol. 39, no. 10, pp. 1482–1493, 1991.

[3] J. Elson, L. Girod, and D. Estrin, "Fine-grained network time synchronization using reference broadcasts," *SIGOPS Oper. Syst. Rev.*, vol. 36, no. SI, pp. 147–163, 2002.

[4] S. Ganeriwal, R. Kumar, and M. B. Srivastava, "Timing-sync protocol for sensor networks," pp. 138–149, 2003.

[5] Y.-C. Wu, Q. Chaudhari, and E. Serpedin, "Clock synchronization of wireless sensor networks," *IEEE Signal Processing Magazine*, vol. 28, no. 1, pp. 124–138, 2010.

[6] J. He, P. Cheng, L. Shi, and J. Chen, "Time synchronization in wsns: A maximum value based consensus approach," in *2011 50th IEEE Conference on Decision and Control and European Control Conference*, pp. 7882–7887, Dec 2011.

[7] Y. Kikuya, S. M. Dibaji, and H. Ishii, "Fault tolerant clock synchronization over unreliable channels in wireless sensor networks," *IEEE Transactions on Control of Network Systems*, pp. 1–1, 2018.

[8] R. Carli, A. Chiuso, L. Schenato, and S. Zampieri, "A pi consensus controller for networked clocks synchronization," *IFAC Proceedings Volumes*, vol. 41, no. 2, pp. 10289–10294, 2008.

[9] R. Carli and S. Zampieri, "Network clock synchronization based on the second-order linear consensus algorithm," *IEEE Transactions on Automatic Control*, vol. 59, pp. 409–422, Feb 2014.

[10] S. Phillips, Y. Li, and R. G. Sanfelice, "A hybrid consensus protocol for pointwise exponential stability with intermittent information," *IFAC-PapersOnLine*, vol. 49, no. 18, pp. 146–151, 2016.

[11] R. Goebel, R. G. Sanfelice, and A. R. Teel, *Hybrid Dynamical Systems: Modeling, Stability, and Robustness*. Princeton University Press, 2012.

[12] F. Ferrante, F. Gouaisbaut, R. G. Sanfelice, and S. Tarbouriech, "State estimation of linear systems in the presence of sporadic measurements," *Automatica*, vol. 73, pp. 101 – 109, 2016.

[13] R. Olfati-Saber and R. M. Murray, "Consensus problems in networks of agents with switching topology and time-delays," *IEEE Transactions on Automatic Control*, vol. 49, pp. 1520–1533, Sept 2004.

[14] J. A. Fax and R. M. Murray, "Information flow and cooperative control of vehicle formations," *IEEE Transactions on Automatic Control*, vol. 49, pp. 1465–1476, Sep. 2004.

[15] C. D. Godsil and G. F. Royle, *Algebraic Graph Theory*. 2001.

[16] K. Narendra and A. Annaswamy, "A new adaptive law for robust adaptation without persistent excitation," *IEEE Transactions on Automatic Control*, vol. 32, pp. 134–145, February 1987.